

# ASSESSING CONSERVATION TREATMENTS OF THE MAIN FAÇADES OF MEDINET HABU TEMPLE, LUXOR–EGYPT

By

**Ahmed Mancı**

Lecture at Department of Restoration and Conservation of Antiquities, Faculty of Archaeology and Tourism  
Guidance, Misr University for Science and Technology, Egypt

## ABSTRACT

[AR]

تقييم علاج وصيانة الواجهات الرئيسية لمعبد مدينة هابو، الأقصر – مصر

تُرکز هذه الورقة على المخاطر البيئية التي تؤثر على النقوش الجدارية بالواجهات الرئيسية للمعبد الجنائزي لرمسيس الثالث بالضفة الغربية للأقصر، مع اقتراح أفضل المواد لحفظ هذه النقوش. لتحقيق هذا الغرض تمت دراسة مواد البناء المستخدمة في المعبد، ونواتج التلف، والعوامل البيئية المحيطة. تم تحديد خصائص المواد من خلال الفحص البصري، والميكروسكوب المستقطب، والميكروسكوب الإلكتروني الماسح المزود بوحدة التحليل العنصري للأشعة السينية، وحيود الأشعة السينية (XRD)، وقياس التغيرات اللونية، وقياس زاوية التلامس مع الماء الثابت، مع تحديد بعض الخصائص الفيزيائية والميكانيكية. أظهرت النتائج أن النقوش الجدارية على الواجهات الرئيسية للمعبد في حالة خطيرة من الحفظ، حيث تأثرت بالعديد من مظاهر وأنماط التلف نتيجة تأثير العديد من عوامل التلف البيئية التي تأتي نتيجة التوسع الحضري والزراعي حول منطقة المعبد، علاوة على الأنشطة البشرية وعوامل التدهور البيولوجي. أظهرت النتائج التي تم الحصول عليها بطرق الفحص والتحليل أن مواد البناء الأساسية هي الحجر الرملي و المونة الجبسية. أظهرت نتائج الدراسة التجريبية للعلاج أن الكمادات المحضرة (A) والتي تتكون من 1000 مل من الماء المقطر، و60 جم من كربونات الأمونيوم، و60 جم من بيكربونات الصوديوم، و25 جم من حمض إيثيلين ديامين رباعي الخليك (إديتا)، و40 جم أربوسيل (لب السليلوز)، هي الأكثر فعالية في إزالة الإتساخات والبقع وفضلات الطيور من أسطح النقوش الجدارية. بالإضافة إلى ذلك، فإن منتج ميثيل ترائي ميسوكسي سيلان له كفاءة كبيرة في تقوية وحماية الحجر الرملي. أيضاً المونة (C) المكونة من (رمال صفراء 100 مل، و جير مطفى 100 مل، ومسحوق حجر رملي رمادي 100 مل، ومسحوق حجر رملي بني 100 مل، وماء مقطر + Eucopr M 5ml). هي أفضل مونة لملاء الفجوات والعراميس في الواجهات الرئيسية للمعبد.

[EN]

This paper focuses on the environmental hazards affecting the wall reliefs at the main facades of the mortuary temple of Ramesses III at Luxor west bank, abreast with proposing the optimum materials to conserve these inscriptions. To achieve the aforementioned purpose; the building materials used in the structure, the deterioration products, and ambient environmental factors were studied. The materials were characterized by visual observations, polarized light microscope, scanning electron microscopy with energy dispersive X-ray spectroscopy (SEM-EDX), X-ray diffraction (XRD), colorimetric measurements, and static water contact angle, with some physical and mechanical properties. The results revealed that the wall reliefs on the main facades of the temple are in a serious preservation state, where affected by several deterioration phenomena and patterns of damage due to the effectiveness of many environmental deterioration factors, which come as a result to urban and agriculture sprawling around the temple area, moreover human activities and biodeterioration factors. The results obtained by investigation and analytical methods revealed that the main building materials are the sandstone and gypsum mortar. The experimental study results of the treatments demonstrated that the prepared poultice (A), which consists of 1000 ml of distilled water, 60g of ammonium carbonate, 60g of sodium bicarbonate, 25g of ethylene diamine tetraacetic acid, and 40g of arbocel (cellulose pulp), is the most effective in removing dirt, stains, and bird droppings from the surfaces of wall reliefs. Additionally, the product of Methyltrimethoxysilane (MTMOS) has a significant efficiency in consolidation and protection of sandstone compared to the other evaluated products in the study. Also, the mortar (C), which consisting of (yellow sand 100ml, slacked lime 100ml, gray sandstone powder 100ml, brown sandstone powder 100ml, distilled water + Eucopr M 5ml), is the best mortar for filling gaps and joints in the main facades of the temple.

**KEYWORDS:** Cleaning, consolidation, EDX, Luxor, Medinet Habu, Mortars, sandstone, SEM, Static water contact angle, wall reliefs, XRD.

## I. INTRODUCTION

The mortuary temple at Medinet Habu, was built by Ramesses III (c. 1182–1151 BC). It is considered the nucleus of the entire building project of Medinet Habu, and today it is still the centre and its dominant feature. It is also the only structure still relatively fully preserved among the surrounding ruins. The temple is located on Luxor's west bank (25° 42' N, 32° 36' E), at the southern extremity of the great necropolis of ancient Thebes, on the desert edge, just above the cultivation [FIGURE 1]<sup>1</sup>. From the geological point, this region is a part of the Stable Shelf, which is characterized by alluvium deposits along the Nile's banks which is of Pliocene age and is bordered by Oligocene, Eocene, and Miocene regions. The Pliocene unit is represented in the study area by two formations, namely, Pliocene fault breccia or intraformational conglomerate and Medamud that are covered by the unconsolidated recent alluvial sediments of a Nile flood plain unit. This unit is composed of two sequential layers: silty clay layer of low shear strength and clay layer, with attaining a total thickness of 18.5 m<sup>2</sup>. The temple was built of sandstone, a sedimentary rock, that highly spreads at the surface of the earth and has been classified according to the kind and proportion of cementitious materials (quartz, calcite, iron oxide, clay or other cements), quartz being the main component that gives it strength. It is commonly described as «Nubian sandstone» because it belongs to the stratigraphic sequence known as the Nubian group. In Egypt, a total of thirty-four ancient sandstone quarries, they occur continuously in the Nile valley and on the adjacent desert plateau from Esan southward into northern Sudan, are identified. In addition, some quarries are located in the western and eastern deserts. The quarries of sandstone at ElSilsilah, ElTaref, Quseir, ElShehab, Kirtas, Duwi, Umm Barmil, Timsah, Abu Aggag and Gabal Ahmar are the most commonly used quarries in ancient Egypt.<sup>3</sup> Sandstone deterioration is a complex process that depends on both internal sandstone characteristics, such as mineral composition, texture, type of cement material, and pore surface formation, as well as external environmental conditions<sup>4</sup>.

Unfortunately, the inscriptions on the main facades of the studied temple are suffering from a bad preservation state, as a result to influence of many deterioration factors like the environmental problems, due to the urban and agriculture sprawling around the temple area. In addition, the effects of biodeterioration factors, the human actions and the effects of climate<sup>5</sup>, where the climate of study area is classified as arid and semi arid. The range of the monthly average air temperature is 12 to 32 °C, while maximum relative humidity (RH%) reaches 50% in December and 29% in August. Average rainfall ranges from 0.01 to 0.2 mm, precipitation is restricted to flash floods. The average wind speed varies between 3.7 and 21.1 km/h, and the evaporation rates are

---

<sup>1</sup> NELSON et Al 1930: 2; HÖLSCHER 1941: 2-4; MURNANE 1980: 1-5; SCOTT 2011: 1-6; JOSÉ DAS 2012: 87.

<sup>2</sup> ELFADALY et Al 2018: 587-610.

<sup>3</sup> NICHOLSON & SHAW 2000: 54-56; HARRELL & STOREMYR 2009: 7-50; LABUS & BOCHEN 2014: 2027-2042; HADI & ALI 2018: 613-619; CAI et Al 2019: 1-18.

<sup>4</sup> MISCEVIC & VLASTELICA 2014: 240-250.

<sup>5</sup> AYMAN et Al 2014: 93-104; ELFADALY et Al 2017: 1-19.

lowest in January (2.5 mm/day) and highest in June (9.4 mm/day)<sup>6</sup>. The effects of those factors can be seen in the aesthetical appearance of the main facades of the temple in many deterioration aspects such as efflorescence, discoloration, scaling, flaking, fragmentation, detachment, powdering, loss of the sandstone's surface layer, microbiological colonization, deposition of guano, and accumulated dust. In addition, can be seen in the effects of internal structural damage in a form of cracking and missing parts. The deterioration of such archaeological buildings as a result of the influence of physical, chemical and biological deterioration factors has been discussed in many works to clarify the mechanism of damage<sup>7</sup>. The treatment that achieves the future preventive effect of such wall reliefs exposed to multiple deterioration agents is always a complex task. Where this requires a broad knowledge of construction materials, previous treatment interventions, conservation materials and techniques as well as an understanding of damage mechanics<sup>8</sup>. The cleaning, consolidation as well as filling gaps and joints are the basic treatment procedures of such wall reliefs in order to restore their appearance before damage, to recover their strength, to increase their durability and to enable regular maintenance especially in an outdoor environment<sup>9</sup>. Many experimental and applied studies have been conducted to demonstrate the effectiveness of multiple techniques and materials in the treatment and conservation of archaeological sandstone buildings<sup>10</sup>. Cleaning treatment is a very delicate process and essential for preservation of archaeological stone buildings. It improves their long term conservation, helps to reveal their aesthetic and artistic values and enhances their historical significance. By removing any undesired material such as dirt, dust, and other harmful materials from their surfaces<sup>11</sup>. The purpose of consolidation treatment is to restore the cohesion between the grains of damaged stones and improve their mechanical properties, which contributes to increasing their durability and helps in the sustainability of the archaeological buildings<sup>12</sup>. Silanes such as methyltrimethoxysilane (MTMOS), tetraethoxysilane (TEOS) and ethyl silicate... etc, are the most well known and successful used in consolidation of sandstone from the late 19<sup>th</sup> century to the present. Where they are commercially available and have excellent properties such as low viscosity, deeper penetration, better consolidation effect, relatively strong, compatibility with sandstone, resists cleavage by ultraviolet solar radiation as well as chemical, thermal and oxidative stability<sup>13</sup>. The completion or filling of missing parts (joints and gaps) is essential to the conservation of archaeological buildings. This treatment has two aims: the first is to support the building, as it suffers from severe weakness in the region of loss and

<sup>6</sup> WÜST & SCHLÜCHTER 2000: 1161-1172; MAHMOUD et Al 2010: 133-142.

<sup>7</sup> GUPTA et Al 2013: 51- 57; LABUS & BOCHEN 2014: 2027 - 2042; BADER 2014: 201-219; HOSSAM 2015: 5-32; EL-GOHARY 2015: 349-36; EL-DERBY 2016: 273-281; VEREZEN 2017: 20-34; BALA'AWI et Al 2018: 49-66; MANSOUR et Al 2019: 1352-1360, CHIAKI et Al 2021: 8-32; AHMED et Al 2021: 53-63.

<sup>8</sup> MOHAMMAD et Al 2019: 3389-3405.

<sup>9</sup> BADER et Al 2016: 103-118.

<sup>10</sup> BADER et Al 2016: 443-458; HELMI et Al 2016: 29- 40; SALEH et Al 2019: 43- 48; REMZOVA et Al 2019: 1-16; CAI et Al 2019: 1-18; YASER et Al 2020: 16-33; HEFNI 2020: 64-75; ORABI et Al 2020: 238-249; GAJDOS et Al 2021, 1-11.

<sup>11</sup> SIEGESMUND et Al 2011: 444; BAGLIONI et Al 2015: 6.

<sup>12</sup> RODRIGUES 2001: 3-14.

<sup>13</sup> GEORGE 2005: 1-14; FERREIRA et Al 2008: 38-53; GABRIELA et Al 2015: 1-6; MARCO & CARLOS 2018: 235-254; REMZOVA et Al 2019: 1-16.

deep erosion; the second is to present the aesthetics and historical values of the building<sup>14</sup>. The conservation principle states that any fill material should be compatible with the original walls in terms of physical, mechanical and optical properties<sup>15</sup>.

**This research aims to:**

- 1-Characterize the used building materials and evaluate the current preservation state of the wall reliefs on the main facades of the mortuary temple at Medinet Habu.
- 2-Propose optimum materials to conserve the inscriptions on the main facades of the temple by conducting experimental studies of treatments, to evaluate the efficiency of two types of prepared poultices, and to determine the best one for removing of dirt, stains and bird droppings from the surfaces of wall reliefs. In addition to evaluate the efficiency of four silicon based consolidation materials, to introduce the most suitable one for consolidation and protection of wall reliefs in the main facade of temple. Such evaluation is carried out on similar sandstone samples collected from the archeological site of Medinet Habu. Also; to evaluate the efficiency of four types of prepared mortars to determine the most suitable one for filling gaps and joints in the main facades of the temple. To achieve such work different examination was carried out to include visual examination, polarizing microscope, scanning electron microscope, X-ray diffraction, and EDX unit (Energy Dispersive X-ray Analysis). The proposed treatment materials were comparatively evaluated by visual examination, colorimetric measurements, static water contact angle, along with determination of some physical and mechanical properties, and morphological characterization by scanning electron microscope.

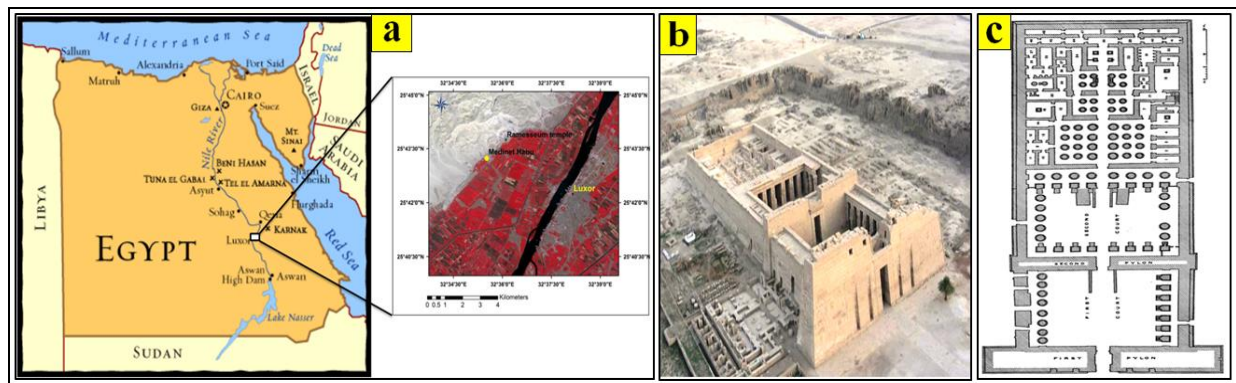


[FIGURE 1] : A) The study area on the Map of Egypt; B) the mortuary temple of Ramesses III in the center of Medinet Habu complex<sup>16</sup>; C) plan of the mortuary temple at Medinet Habu. NELSON et Al 1930: 11.

<sup>14</sup> HASSAN 2022: 38-45.

<sup>15</sup> BALKSTEN 2010: 1-8.

<sup>16</sup> ELFADALY et Al 2018: 587-610.

## II. MATERIALS AND METHODS

### 1. Materials

To characterize the building materials used in the main facades of the studied temple, micro-samples of the stone, mortar joints and salt encrustations were carefully collected from several locations on the walls, especially from the degraded parts as a result of deterioration mechanisms, and they were studied using various investigation and analysis techniques.

For applying the cleaning tests on the main facades of the temple, two types of poultices (A & B) were prepared, their compositions is reported in [TABLE 1].

| Components of Poultice (A)                   | Components of Poultice (B)       |
|--|----------------------------------|
| - 1000 ml distilled water                    | - 1000 ml distilled water        |
| - 60 gm ammonium carbonate                   | - 10 gm ammonium carbonate       |
| - 60 gm sodium bicarbonate                   | - 10 gm sodium bicarbonate       |
| - 25 gm (Ethylene diamine tetra acetic acid) | - 20 gm Carboxy Methyl Cellulose |
| - 40 gm Arbocel (cellulose pulp)             |                                  |

[TABLE 1]: Composition of the prepared A & B cleaning poultices© Done by researcher

Cubic sandstone samples (3.5 cm<sup>3</sup>) were prepared for the experimental study of the consolidation products, according to guidelines for conservation purposes of archaeological surfaces. Four silicon polymers were used for consolidating the prepared sandstone samples. The chemical compositions of the used consolidation materials are reported in [TABLE 2]. To simulate the consolidation process as it happens in the archaeological field, the consolidation materials were spread on the surfaces of sandstone samples by brush until the surface was saturated. Then the treated samples were left at the room temperature and controlled RH 50% for about a month, to complete the polymerization process<sup>17</sup>.

| Product       | Composition                          | Solvent      | Company                |
|---------------|--------------------------------------|--------------|------------------------|
| Wacker OH 100 | Ethyl silicate & methyl ethyl ketone | Acetone      | Wacker Chemie, Germany |
| Estel 1000    | Ethyl silicate                       | White spirit | CTS Italian company    |
| Dow Corning   | Methyltrimethoxysilane (MTMOS)       | Acetone      | Sigma-Aldrich, Germany |
| Nano Estel    | Nano silica                          | Water        | CTS Italian company    |

[TABLE 2]: The chemical compositions of the used consolidation materials© Done by researcher

To prepare the mortars for filling gaps and joints in the main facades of the studied temple, the following materials were used: high quality slaked lime, good quality yellow sand, gray crushed sandstone, brown crushed sandstone, heba powder, Eucopor M product, Addibond product and distilled water. The used sand was free from salts, organic matter, clay, and silt. They were sieved through a medium sieve in order to

<sup>17</sup> LICCIULLI et Al 2011: 437- 444; HELMI et Al 2016: 87-96; MOHAMMAD et Al 2019: 3389-3405.

achieve homogeneous, gradient-grained mixture. The heba powder was obtained by grinding and sifting the clay containing calcitic soil deposits. Eucopor M product is a special plasticiser for mortar, based on neutralized vinsol resin, produced by Swiss Chem. Addibond product is based on styrene-butadiene latex stabilized with polyvinyl alcohol, contains a non-migratory plasticizer and is produced by Chemicals for Modern Building company (CMB). The experimental study was conducted using four types of mortar prepared from the above mentioned materials. Their compositions are reported in [TABLE 3]. The solid components were mixed in dry states, according to the amounts listed in [TABLE 3]. This was followed by mixing the slacked lime in a small quantity of water and adding to the mixture through a fine strainer, then adding the improved materials according to their ratio. Finally mixing the ingredients manually, adding water as needed in order to obtain a suitable texture, then casting fresh mortar in cubic metal moulds (5 cm<sup>3</sup>), with light compaction to obtain well compacted mortar free of air voids. After one day the samples were demoulded carefully, left to set and harden at room temperature in order to carry out the evaluation tests.

| <b>Mortar name</b> | <b>The compositions</b>  |
|--------------------|--|
| (A)                | Yellow sand 100ml + Slacked lime 150ml + Gray sandstone powder 100ml + Distilled water.  |
| (B)                | Yellow sand 100ml + Slacked lime 100ml + Gray sandstone powder 150ml + Brown sandstone powder 50 ml + Distilled water.                               |
| (C)                | Yellow sand 100ml + Slacked lime 100ml + Gray sandstone powder 100ml + Brown sandstone powder 100ml + Distilled water + Eucopor M 5ml                |
| (D)                | Yellow sand 100ml + Slacked lime 100ml + Gray sandstone powder 100ml + Brown sandstone powder 100ml + Heba powder 50ml + Addibond + Distilled water. |

**[TABLE 3]: The compositions of the mortars© Done by researcher**

## 2. Methods

Thin section from the collected sandstone and mortar joints samples were prepared for the petrographic study, which was carried out using Nikon eclipse LV100POL polarizing microscope. Quanta 250 scanning electron microscope (SEM) was used to investigate the surface of archaeological samples and the treated sandstone. Philips analytical X-ray diffractometer was used to determine the mineralogical composition for the collected samples. The operating conditions were gained through Cu k  $\alpha$  radiation.

The spectra were collected from 2-60 (2 $\theta$ ); the scanning speed was 2 $\theta$  = 1 degree/min. at constant voltage 40 kv, and 25 mA. The obtained XRD patterns and relative intensities were compared with the «JCPDS» standards of 1967 to identify the compounds of studied samples<sup>18</sup>. The micro chemical analysis was carried out using EDX unit (Energy Dispersive X-ray Analysis).

<sup>18</sup> JCPDS standards 1967.

The physical properties of the samples were determined by calculating the volume of each sample and weighing the dry and wet weight of each sample<sup>19</sup>.

Bulk Density (D) in g/cm<sup>3</sup> of the samples was measured before and after treatment using the following equation:-

$$D = \frac{W}{V}$$

Where; (D) is the bulk density in g/cm<sup>3</sup>, (W) is original weight in gm and (V) is volume in cm<sup>3</sup>.

Water Absorption (W.A) in % of the samples was measured before and after treatment using the following equation:-

$$W.A = \frac{W_2 - W_1}{W_1} \times 100 = \%$$

Where; (W. A) is the water absorption in %, (W1) dry weight of the sample in g before immersion and (W2) saturation weight of the sample in g after immersion in water for 24 h.

Apparent porosity (A.P) in % of the samples was measured before and after treatment using the following equation:-

$$A.P = \frac{W_2 - W_1}{V} \times 100 = \%$$

Where; (A.P) is the apparent porosity in %, (W1) dry weight in g, (W2) wet weight in g and (V) is volume in cm<sup>3</sup>.

The compressive strength of experimental sandstone samples and the prepared mortar were determined according to ASTM C 170<sup>20</sup>.

A colorimetric study of the experimental samples was carried out by means of Optimatch 3100 spectrophotometer, in order to calculate and determine variation of the aesthetical properties induced by the treatments, according to the following equation:-

$$\Delta E^*_{ab} = \sqrt{[(\Delta L^*)^2 + (\Delta a^*)^2 + (\Delta b^*)^2]}$$

Where L\* is the lightness/darkness coordinate, a\* the red/green coordinate (+a\* indicating red and -a\* green) and b\* the yellow/blue coordinate (+b\* indicating yellow and -b\* blue. While ΔL\*, Δa\* and Δb\* are the differences in the, L\*, a\* and b\* coordinates (according to CIELAB color space) of the treated and untreated samples<sup>21</sup>.

The hydrophobicity of the experimental sandstone samples was evaluated using Drop master DM-701, by measuring the static water contact angle with samples, fully automated.

<sup>19</sup> HEMEDA et Al 2018: 835-846.

<sup>20</sup> ASTM C 170 1976.

<sup>21</sup> CIE Standard S014-4/E 2007; DARWISH 2013: 413-422; BADER et Al 2016: 443-458.

### III. RESULTS AND DISCUSSION

#### 1. State of Preservation

Visual examination confirmed that the wall reliefs at the main facades of the mortuary temple of Ramesses III were highly influenced by many deterioration patterns and forms, as follows: -

A lot of the sandstones have lost their inscriptions due to scaling and flaking [FIGURE 2/A-B]. This type of decay can be caused as a result of using sandstone blocks after carving; and the stones are laid so that the bedding planes of the rock are vertical rather than horizontal, which allows moisture to flow through the blocks freely<sup>22</sup>. This stimulates salt weathering by crystallization pressures of salts between its sedimentation layers<sup>23</sup>. Moreover, there is powdering on the surfaces of sandstones saturated with moisture, which are located primarily in some lower parts until 3 meters height of the external facades, resulting in the loss of inscriptions [FIGURE 2/ A, C]. Powdering is one of the most common deterioration forms to sandstone. This is due to the weakness or loss of the cement materials of the mineral granules, as a result to some deterioration factors such as air temperature (AT) and relative humidity (RH), by their alternative cycles and salt weathering<sup>24</sup>. Also discoloration took place at some parts of the stone blocks [FIGURE 2/ D, F], may be due to many factors such as moisture, fire and oxidation of oxidants especially iron oxides as a result of chemical weathering by free oxygen and water. In normal temperatures, free oxygen reactions are slow; while oxidative processes accelerate in the presence of water that is likely to dissolve some minerals, transfer to the surface of the temple walls and then evaporate, which leave disfiguring reddish brownish stains of the inscriptions<sup>25</sup>. Multiple types of cracks are clearly visible by the naked eye, such as individual horizontal, vertical cracks and networks of cracks [FIGURE 2/ G, H]. They vary in length and depth, and can lead to fragmentation of the stone into small pieces. The most widely discussed reason in studies is that the mechanical stress that occurs by salts due to the growth of hydration pressure of the saline solution inside the stone pores constitutes a great pressure that leads to cracks<sup>26</sup>. Fragmentation, observed in many sandstones [FIGURE 2I], occurs as a result to effects of the mechanical and the physiochemical processes, depending on properties of sandstone, the mineral composition, texture, pore surface formation<sup>27</sup>. There is an extensive amount of dust layer adhered tightly to the inscriptions [FIGURE 2J]. This layer had turned into a layer of mud in some surfaces, which was saturated of moisture. Also, the presence of many kinds of surface deposits such as bird droppings, especially pigeon excrements, and wasp's nests, adhered tightly causing staining of the stone surfaces, and distortion of the inscriptions [FIGURE 2/ K, L]. The deposits represent chemical and biological deterioration factors; through creating some

---

<sup>22</sup> SWANN 24-29.

<sup>23</sup> BADER et Al 2016: 103-118, GERMINARIO & OGUCHI 2021: 85-93.

<sup>24</sup> DESARNAUD et Al 2015: 1- 10; LAMP et Al 2016: 1-24.

<sup>25</sup> NORD 1993: 24- 35; ZHIXUE et Al 2010: 543-551; BADER 2014: 201-219.

<sup>26</sup> EPPES et Al 2017: 470- 508.

<sup>27</sup> MISCEVIC et Al 2014: 240-250; YÜKSEK 2019: 1-13.



acidic central points on sandstone surfaces<sup>28</sup>. Many forms of salts have been observed on the external facades of the studied temple such as (hard crusts and efflorescence) [FIGURE 2/ M, O]. The salts accumulation may be related to presence of salt in the soil, previous intervention using Portland cement mortar, and the rising salty ground water level in the temple area, as a result to the unplanned urban which is associated with bad sewage networks, and the agricultural encroachment associated of poor irrigation water management<sup>29</sup>. As the groundwater level rises, dissolved salts move with the water into the pores and cracks of sandstones. After the water evaporates salt crystals accumulate on the surface of the stone (efflorescence) and the subsurface of the stone (sub-efflorescence and crypto-efflorescence). The scaling, spalling, powdering and cracking, are some physical degradation forms that affect the archaeological buildings of sandstone, as a result to the effects of salt weathering<sup>30</sup>. The red bricks were used to rebuild areas that lacked the original sandstone and the damaged areas in the external facades had been patched with black cement mortar, which caused darkening, cracking on the surrounding sandstones, and salt crystals accumulation [FIGURE 2/ P, Q]. Most joints in the external facades are missing the original mortar [FIGURE 2/R]. Different types of intentional mechanical damage were recorded due to the human activity which includes, blessing marks (knife whetting), and gaps over wide areas. Moreover, on the lower blocks, there are many loops that had been carved from the Middle Ages until the last century, for securing animals [FIGURE 2/ S &U].

---

<sup>28</sup> EL-GOHARY 2015: 349-368; SPENNEMANN et Al 2017: 2-15; SPENNEMANN et Al 2017: 19-28; SPENNEMANN et Al 2018: 15-28; AHMED et Al 2021: 53-63; MOUSSA et Al 2021: 1-16.

<sup>29</sup> WÜST & SCHLÜCHTER 2000: 1161-1172; MOUSSA 2007: 172; MOUSSA et Al 2007: 1-11; ELFADALY et Al 2017: 1-9.

<sup>30</sup> BENAVENTE et Al 2004: 532-544; SMITH et Al 2008: 275-282; YALDIZ 2010: 1-10; AYMAN et Al 2014: 93-104; ELFADALY et Al 2017: 2-19; ELFADALY et Al 2018: 587- 610; TORRES 2018: 560-570; MANSOUR et Al 2019: 1352-1360; GERMINARIO & OGUCHI 2021: 85-93; MARTINEZ et Al 2021: 123- 132.

*ASSESSING CONSERVATION TREATMENTS OF THE MAIN FAÇADES OF  
MEDINET HABU TEMPLE, LUXOR-EGYPT*

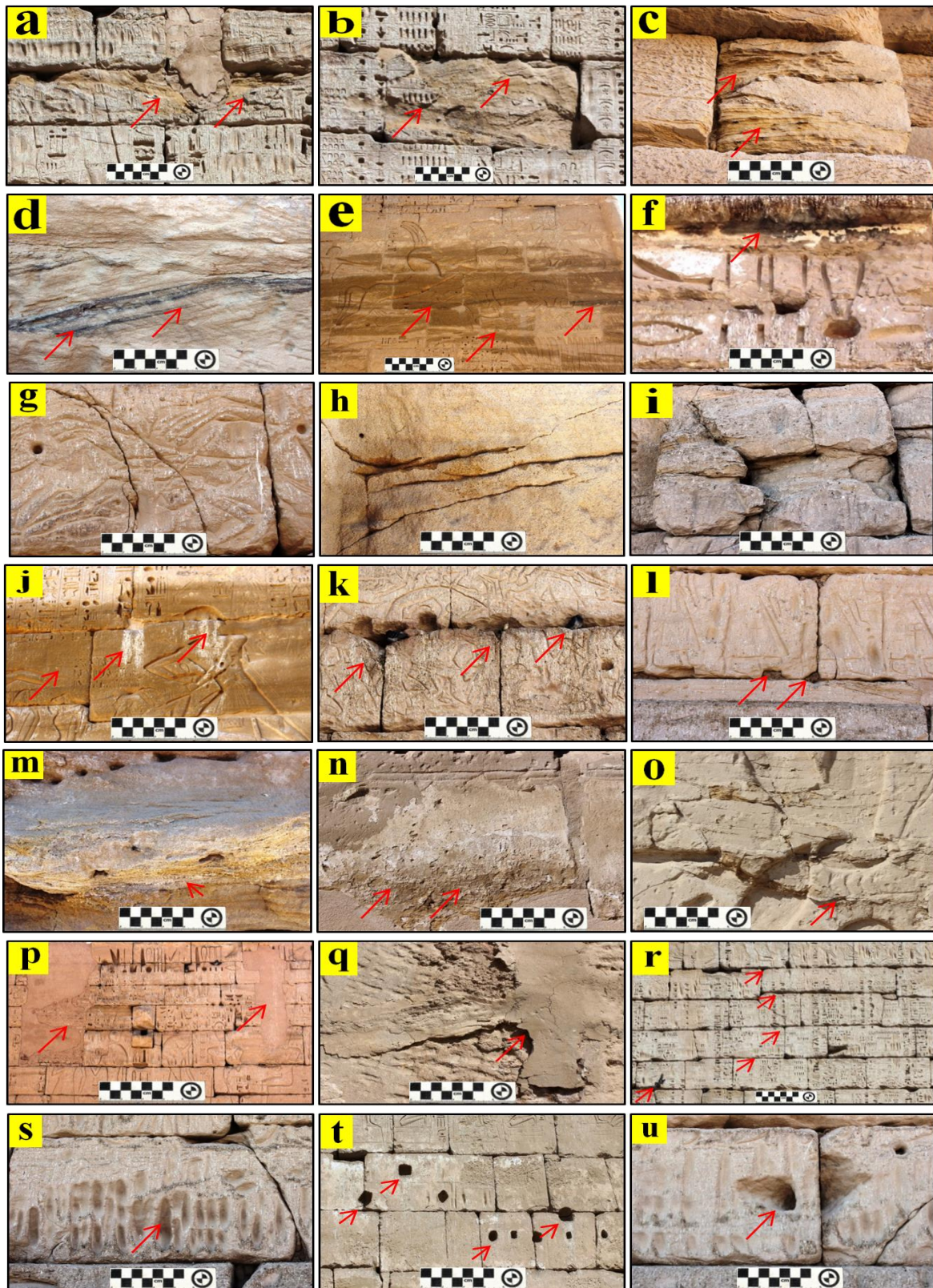


[FIGURE 2]: Preservation state of the external facades of the mortuary temple at Medinet Habu. A) scaling and powdering; B) scaling, flaking, and powdering; C) powdering in wet areas; D) discoloration by oxidation of iron oxides; E) discoloration by moisture; F) discoloration by fire; G) horizontal cracks; H) vertical cracks; I) fragmentation; J& K) dust layer adhered and bird droppings; L) wasps' nest; M) details of efflorescence; N) salt crust; O) micro cracks as a result sub-efflorescence, and crypto-efflorescence; P& Q) previous intervention by red brick and cement mortar; R) loss of joints mortar; S) intentional blessing marks (knife whetting); T) intentional gaps; U) loops for securing animals.

## 2. Characterization of Building Materials

The petrographic study revealed that the studied archaeological sandstone sample was composed mainly of quartz as an essential constituent, with minor amounts of clay minerals (kaolinite) and calcite, in addition to traces of biotite, feldspars, zircon, iron oxides, and opaques. Quartz occurs as sub rounded to angular, very fine to medium and sorted grains. Most of the quartz grains are monocrystalline while few are polycrystalline. Some grains are cracked and fractured. Feldspars occur as sub angular to angular grains. Clay minerals occur as cement material in most parts, while calcite occurs as cement material in some parts [FIGURE 3/A & B]. The components and features of studied sandstone sample are the same components and properties of Nubian sandstone, from Gebel El- Silsila in south -western Egypt (about 160 km south of Luxor, 50 km north of Aswan)<sup>31</sup>.

The petrographic study revealed that the mortar's joints sample is formed mainly of gypsum, fragments of carbonate rock in micrite form, quartz (sand grains), in addition to a minute amount of iron oxides and opaques. Quartz presents a single very fine to medium grained, subrounded to sub angular grains scattered in the matrix. Gypsum occurs as micro flakes. Rock fragments are fine to medium grained and have rounded to sub angular outlines. Gypsum and very tiny carbonate crystals make up the sample matrix [FIGURE 3/ C & D]. This finding confirms that the mortars in ancient Egypt were basically formed of processed gypsum, crushed limestone and sand<sup>32</sup>. Mortar was employed in Egyptian construction techniques to fill in the spaces between blocks, it was not important for bonding the heavy stone components, due to its low parameters of mechanical resistance<sup>33</sup>.

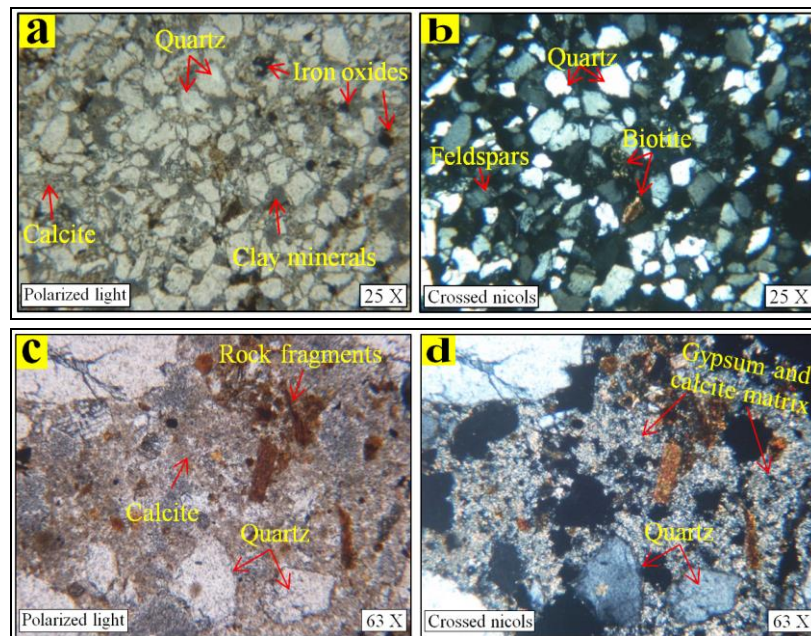


[FIGURE 3]: Petrographic microphotographs of sandstone and joint mortar samples; A) sandstone under plane polarized light (PPL); B) sandstone under cross polarized light (CPL); C) mortar's joints under plane polarized light (PPL); D) joint mortar under cross polarized light (CPL).

<sup>31</sup> FITZNER et Al 2003: 1089-1103.

<sup>32</sup> MOUSSA et Al 2009: 292-308.

<sup>33</sup> DZIEDZIC et Al 2015: 93-111.

SEM examination of sandstone samples at the exterior facades of the studied temple revealed variable sizes of angular and subrounded quartz grains [FIGURE 4/A]. In addition, the growth of salt crystals between the quartz grains led to a collapse of sandstone's internal structure and the dissolution of cement materials. These effects caused loss cohesion among stone particles, an increase in porosity as obviously observed in SEM photomicrograph [FIGURE 4/A]. It also revealed some mechanical deformations to the quartz grains, such as micro exfoliation, micro pitting and breaking as obviously observed in SEM photomicrograph [FIGURE 4/B]. SEM photomicrographs [FIGURE 4/C, D&E] revealed the dense coats of halite crystals on the stone surface. In SEM photomicrograph halite appears as salt crust [FIGURE 4/C], large euhedral cubic aggregates [FIGURE 4/D], in addition to prism and needles [FIGURE 4/E]. The SEM examination of the mortar's joints sample from the external facades of the temple revealed variable sizes (very fine to fine to medium grained) of rounded to sub rounded and subangular particles of quartz grains. Diffusion of salt crystals between the grains, disintegration of granules and loss of cohesion, as a result to dissolution and loss of cement materials, led to an increasing porosity as obviously observed in SEM photomicrograph [FIGURE 4/F].

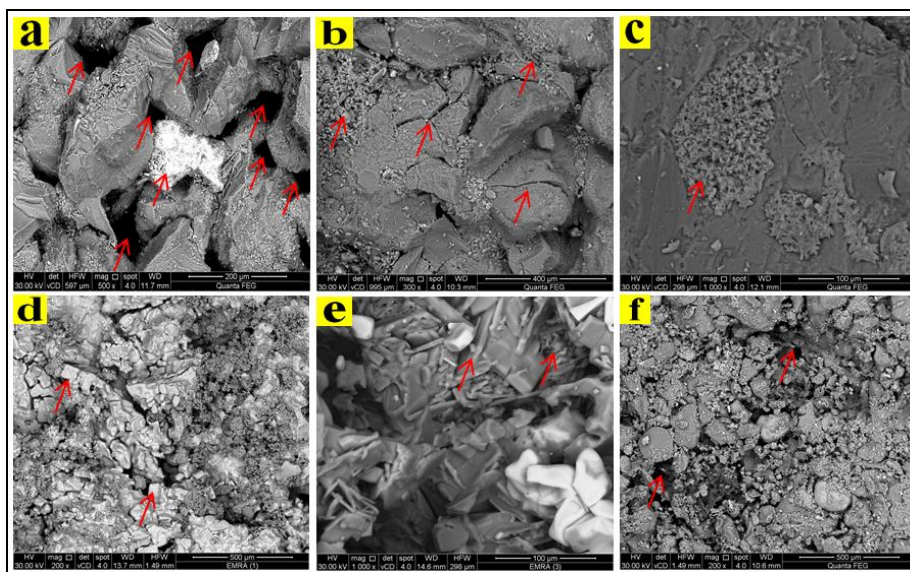


[FIGURE 4]: SEM micrographs of building materials samples; A) show angular and sub rounded grains of quartz, dissolution of cement materials which led to an increasing in porosity of sandstone and presence of sodium chloride crystals between quartz grains; B) mechanical deformations to the quartz grains (micro exfoliation, micro pitting and breaking); C, D & E) dense coats of halite crystals covering the stone surface; F) SEM micrographs of mortar's joints sample.

#### The results of X-ray diffraction revealed the following:-

- The studied sandstone samples [FIGURE 5/A & B] consist mainly of quartz  $\text{SiO}_2$ , kaolinite  $\text{Al}_2(\text{OH})_4\text{Si}_2\text{O}_5$ , calcite  $\text{CaCO}_3$  and halite  $\text{NaCl}$ . Although rare amounts of biotite, feldspars, zircon, iron oxides and opaques were detected by polarizing microscope, they were not detected by XRD due to their very low proportions in the sample.
- The mortar's joints sample [FIGURE 6/A] consists mainly of gypsum  $\text{CaSO}_4 \cdot 2\text{H}_2\text{O}$ , calcite  $\text{CaCO}_3$ , quartz  $\text{SiO}_2$  and halite  $\text{NaCl}$ .

- The salt sample [FIGURE 6/B] indicated that it is mainly consists of halite. The presence of halite within sandstone and mortar's joints components indicates a high weathering has occurred, as clearly observed by SEM, which caused by the mechanical stress resulted by the crystallization cycles of halite salt<sup>34</sup>. These results match very well with the petrographic study and SEM.

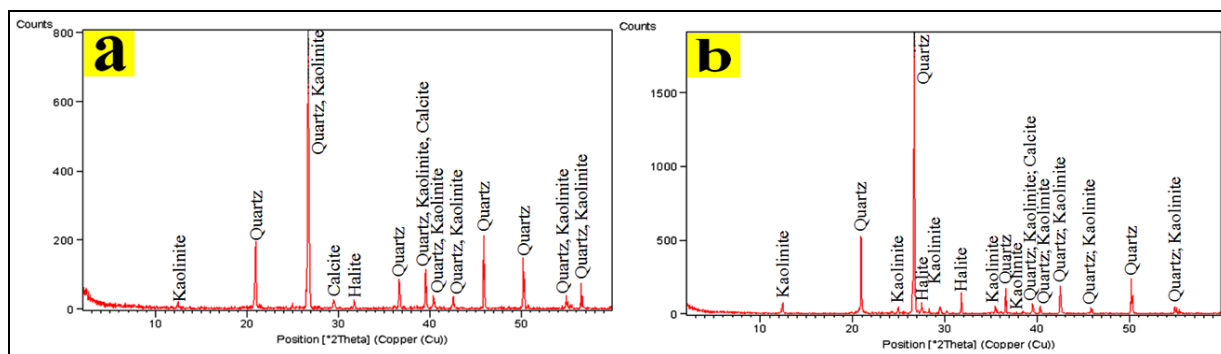


[FIGURE 5]: A& B) XRD pattern of the sandstone samples from the external facades of the temple.

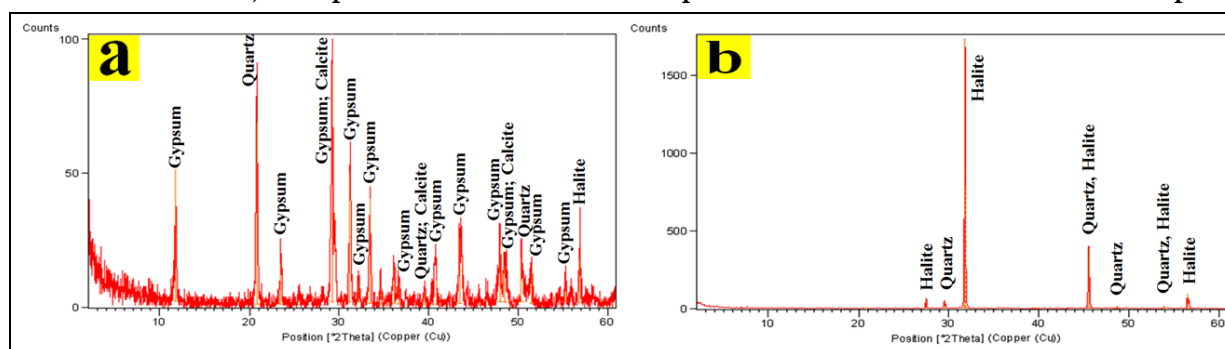


[FIGURE 6]: A) XRD pattern of mortar's joints sample; B) XRD pattern of salt sample.

The EDX analysis of the studied sandstone and mortar's joints samples [FIGURE 7] were carried out to identify the main elements contained in the samples. EDX spectrum of sandstone sample [FIGURE 7/A] revealed the presence of silicon (39.63%), aluminum (3.78%), oxygen (45.37%), calcium (2.90%), carbon (5.61%), chlorine (1.05%), sodium (0.84%) and iron (0.82%). The high peaks of silicon and oxygen confirmed the existence of silicon dioxide (quartz,  $\text{SiO}_2$ ) as the main component of the sample. An aluminum and silicon peak implies the presence of aluminosilicate materials (e.g., clays «kaolinite,  $\text{Al}_2(\text{OH})_4\text{Si}_2\text{O}_5$ »). The peaks of carbon and calcium indicate the existence of carbonate mineral (calcite,  $\text{CaCO}_3$ ). Small intensity peak of iron refer to the presence iron oxide. The peaks of chlorine and sodium proved the presence of halite (Sodium Chloride,  $\text{NaCl}$ ) in the sample. This result confirm the results of XRD.

EDX spectrum of mortar's joints sample [FIGURE 7/B] revealed the presence of silicon (8.33%), aluminum (1.37%), oxygen (43.94%), calcium (26.09%), sulfur (10.86%), carbon (5.47%), chlorine (1.46%), sodium (1.06%), and iron (1.42%). The high peaks of calcium, sulfur and carbon indicates the existence of calcium carbonates (calcite,  $\text{CaCO}_3$ ) and calcium sulphates (gypsum  $\text{CaSO}_4 \cdot 2\text{H}_2\text{O}$ ). The high peaks of silicon and oxygen confirmed the existence of silicon dioxide (quartz,  $\text{SiO}_2$ ). The peaks of chlorine and sodium proved

<sup>34</sup> RUFFOLO et Al 2013: 753-758.

the presence of halite mineral (Sodium Chloride, NaCl) in the sample. It was suggested that the presence of aluminum, and iron arised from the clay minerals impurities in the fragments of stone or the soiling materials.

The analysis results that were obtained using XRD and EDX confirmed the results obtained by petrographic and morphologic studies.

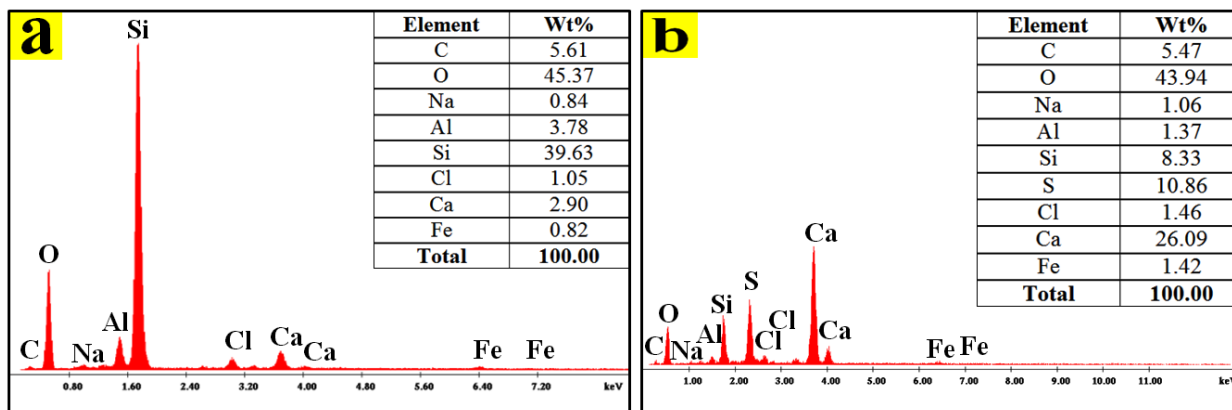


[FIGURE 7]: A) EDX spectrum of sandstone sample; B) EDX spectrum of the mortar's joints sample.

### 3. Evaluation of Conservation Treatments

#### A. Evaluation of the Cleaning Treatment

The experimental study of cleaning materials and techniques was carried out directly on the southern facade of the temple, where the inscriptions suffer greatly from effects of accumulated dust and bird droppings, especially pigeon droppings. For this purpose, the poultice technique was chosen because it allowed for proper control of all stages, ensuring complete removal of undesired materials while preventing them from penetrating the pores of sandstone. Two types of poultices were prepared. The first poultice (A) compositions were mixed according to the percentages mentioned in [TABLE 1] with 40 mg Arbocel (cellulose pulp). The second poultice (B) compositions were mixed according to the percentages mentioned in table (1) with 20 mg of Carboxy Methyl Cellulose. Both composites were applied on a thin sheet of Japanese paper over the surface of the dirt, to avoid the adhesion of the poultice to the stone surface. The poultices were applied in the morning to keep them moist for a longer time. The application time for each poultice was one hour. Finally; the poultices were removed in successive stages, after each stage remaining solubilized materials were removed using a cotton swab embedded with distilled water, until complete removal of poultices. The visual observations reveal that the cleaning proceeded by the poultice (A) gave good results, where the layer of dirt was completely disintegrated, which allowed it to be easily removed. But the dirt was not completely dissolved after removing the poultice (B), which required repeating the poultice three times to obtain the same result that was obtained with one application of poultice (A) [FIGURE 8].

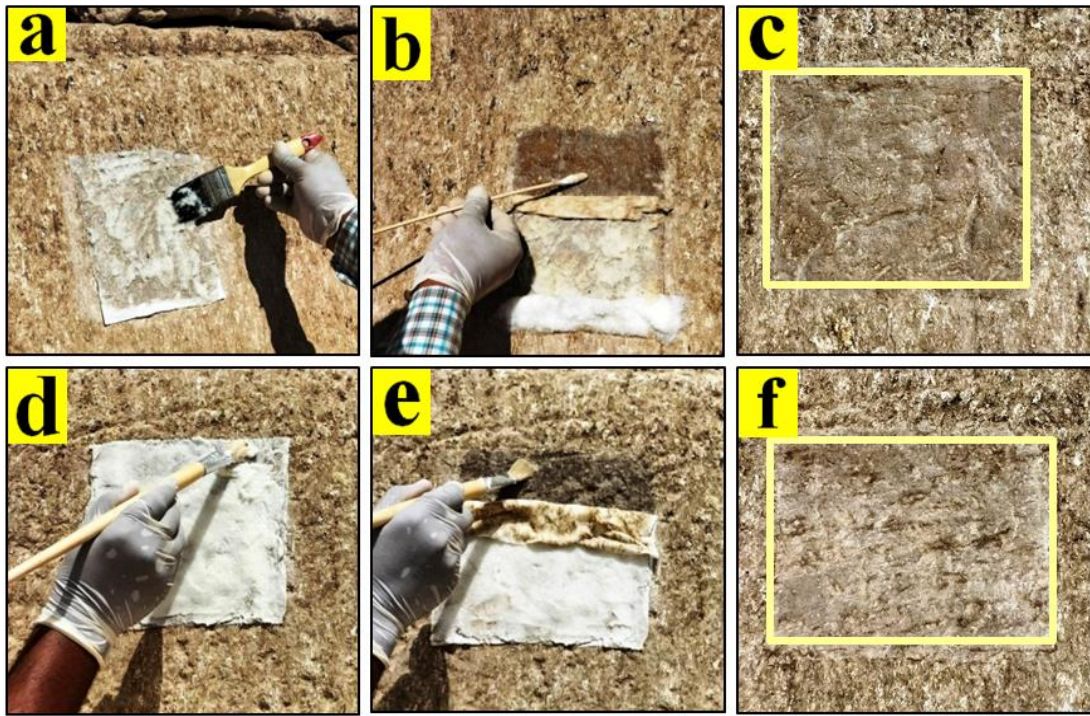


[FIGURE 8]: The cleaning of the accumulated dust and bird droppings on the inscriptions. A& B) application of the poultice (A); C) the cleaning result after removing the poultice (A); D& E) application of the poultice (A); F) the cleaning result after removing the poultice (B).

## B. Evaluation of Consolidation Materials

### 1. Scanning electron microscope (SEM)

SEM micrographs of the treated sandstone samples [FIGURE 9] revealed that all the consolidants utilised in this study succeeded in consolidating the samples with varying degrees, except for the Nano Estel product. Sample treated with Wacker OH 100 [FIGURE 9/A] illustrated that the consolidant filled the pores, improving the connection between the grains, and it formed a superficial layer full of micro cracks, obscured many of the individual particles. Sample treated with MTMOS [FIGURE 9/B] illustrated that the consolidating material surrounded the particles, filled the big and small pores and coated the surfaces of the sample with a homogenous polymeric layer without blocking the pores.

Also; individual particles are visible. Sample treated by Estel 1000 [FIGURE 9/C] illustrated that the consolidant filled most pores, covered the samples with rough homogenous polymeric network, and containing micro cracks in some parts. The sample treated with Nano Estel [FIGURE 9/D] illustrated that the consolidation material covered the surfaces of the sample with an inhomogeneous dense coating containing tiny individual nanoaggregates and filled large cracks.

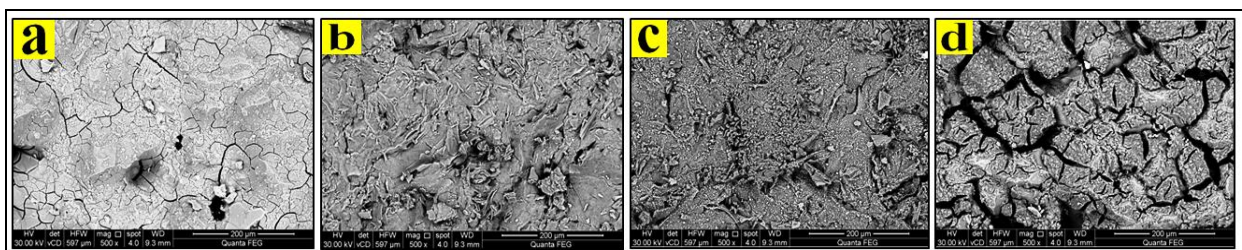


[FIGURE 9]: SEM Micrographs of the treated sandstone samples; A) Wacker OH 100 treatment; B) MTMOS treatment; C) Estel 1000 treatment; D) Nano Estel treatment.

## **2. Physical and Mechanical Properties**

Improving the physical and mechanical properties of treated sandstone samples is an important goal to be achieved with the use of consolidation products. By measurement, it was found that all the consolidation materials used in the study achieved this goal, where they all resulted in an increase in bulk density, a decrease in both apparent porosity and water absorption to varying degrees. The results were reported in [TABLE 4 & FIGURE 10]. By comparison, it was found that the material (MTMOS) achieved the best results in improving the physical and mechanical properties of the treated samples, as follows:

**Bulk density:** the treated samples with MTMOS, achieved the highest bulk density of 2.11 g/cm<sup>3</sup>, which is higher than the untreated sample by about 11.64% that was 1.89 g/cm<sup>3</sup>. The treated samples with Estel 1000 ranked second, achieved bulk density of 2.08 g/cm<sup>3</sup>, which was higher than the untreated sample by about 10.05%, while the treated samples with Wacker OH 100 ranked third, achieved bulk density of 2.05 g/cm<sup>3</sup> which was higher than the untreated sample by about 8.46%. The treated samples with Nano Estel achieved lowest bulk density of 2.02 g/cm<sup>3</sup>, but were still higher than the untreated sample by about 6.87%.

**Apparent porosity:** the treated samples with MTMOS, achieved the best result in reducing the rates of apparent porosity. It gave the lowest average values of apparent porosity, amount to 0.78% which lowers than the untreated sample by about 96.57% which was 22.78%. But the treated samples with Estel 1000, ranked second in reducing the rates of apparent porosity, where it achieved average values of apparent porosity 14.72%, and its decrease ratio due to consolidation treatment was only 35.38%. The treated samples with Wacker OH 100 ranked third in reducing the rates of apparent porosity, where it achieved average values of apparent porosity 13.09%, and its decrease ratio due to consolidation treatment was only 42.53%. While the treated samples with Nano Estel ranked last in reducing the rates of apparent porosity, where it achieved average values of apparent porosity 21.7%, and its decrease ratio due to consolidation treatment was only 4.74%.

**Water absorption:** the treated samples with MTMOS, achieved the best result in reducing the amount of water absorption. It gave the lowest average values of water absorption, which measured 0.39% and was lower than the untreated sample that measured 96.75%, and its decrease was by about 96.75%. This low percentage can be attributed to that the MTMOS product is a hydrophobic material. The treated samples with Estel 1000, ranked second in reducing the rates of water absorption, where it achieved average values of water absorption 7.12%, and its decrease ratio due to consolidation treatment was only 40.61%. The treated samples with Wacker OH 100 ranked third in reducing the rates of water absorption, where it achieved average values of water absorption 6.38%, and its decrease ratio due to consolidation treatment was only 46.78%. While the treated samples with Nano Estel ranked last in reducing the rates of water absorption, where it achieved average values of water absorption 10.84%, and its decrease ratio due to consolidation treatment was only 10.34%.



Compressive Strength: the treated samples with MTMOS achieved the best result in increasing the compressive strength, where it gave highest average values of compressive strength of 211.66 kg/cm<sup>2</sup>, by an increase of 95.98% with respect to untreated samples, which achieved average values of compressive strength 108 kg/cm<sup>2</sup>. The treated samples with Estel 1000 ranked second in increasing the rates of compressive strength, where it achieved average values of compressive strength 193kg/cm<sup>2</sup>, and its increase ratio due to consolidation treatment was only 78.70%. The treated samples with Wacker OH 100 ranked third in increasing the rates of compressive strength, where it achieved average values of compressive strength 197kg/cm<sup>2</sup>, and its increase ratio due to consolidation treatment was only 82.41%. While the treated samples with Nano Estel ranked last in increasing the rates of compressive strength, where it achieved average values of compressive strength 112.33kg/cm<sup>2</sup>, and its increase ratio due to consolidation treatment was only 4.01%.

This result may be attributed to low viscosity rate of the methyltrimethoxysilane polymer, which enables it to high and easy penetration into the porous matrix, in addition to high and fast reactivity in the treated zones, in addition to its high compatibility with sandstone samples, where the methyltrimethoxysilane polymer is hydrolysed with water to form silanols which then polymerize in a condensation reaction to form a polymer that increases the cohesion of the stone material<sup>35</sup>.

---

<sup>35</sup> FERNANDEZ et Al 2017: 1-18.

*ASSESSING CONSERVATION TREATMENTS OF THE MAIN FAÇADES OF  
MEDINET HABU TEMPLE, LUXOR-EGYPT*

| Tested Property                            | Samples                            | Results |       |       |         |
|--|------------------------------------|---------|-------|-------|---------|
|  |                                    | S1      | S2    | S3    | Average |
| Bulk density (g/cm <sup>3</sup> )          | Untreated                          | 2.04    | 2.04  | 2.15  | 2.08    |
|  | Treated with Wacker OH 100         | 2.09    | 2.03  | 2.03  | 2.05    |
|  | Increase in bulk density %         |         |       |       | 8.46    |
|  | Treated with MTMOS                 | 2.02    | 2.13  | 2.18  | 2.11    |
|  | Increase in bulk density %         |         |       |       | 11.64   |
|  | Treated with Estel 1000            | 2.04    | 2.04  | 2.15  | 2.08    |
|  | Increase in bulk density %         |         |       |       | 10.05   |
|  | Treated with Nano Estel            | 2.02    | 2.03  | 2.01  | 2.02    |
|  | Increase in bulk density %         |         |       |       | 6.87    |
| Apparent porosity (%)                      | Untreated                          | 22.76   | 22.78 | 22.80 | 22.78   |
|  | Treated with Wacker OH 100         | 13.11   | 12.52 | 13.63 | 13.09   |
|  | Decrease in apparent porosity %    |         |       |       | 42.53   |
|  | Treated with MTMOS                 | 0.67    | 0.74  | 0.93  | 0.78    |
|  | Decrease in apparent porosity %    |         |       |       | 96.57   |
|  | Treated with Estel 1000            | 16.78   | 13.63 | 13.74 | 14.72   |
|  | Decrease in apparent porosity %    |         |       |       | 35.38   |
|  | Treated with Nano Estel            | 21.48   | 21.85 | 21.77 | 21.7    |
|  | Decrease in apparent porosity %    |         |       |       | 4.74    |
| Water absorption (%)                       | Untreated                          | 11.86   | 11.99 | 12.11 | 11.99   |
|  | Treated with Wacker OH 100         | 6.28    | 6.15  | 6.70  | 6.38    |
|  | Decrease in water absorption %     |         |       |       | 46.78   |
|  | Treated with MTMOS                 | 0.33    | 0.38  | 0.48  | 0.39    |
|  | Decrease in water absorption %     |         |       |       | 96.75   |
|  | Treated with Estel 1000            | 8.23    | 6.65  | 6.49  | 7.12    |
|  | Decrease in water absorption %     |         |       |       | 40.61   |
|  | Treated with Nano Estel            | 10.62   | 10.7  | 10.84 | 10.75   |
|  | Decrease in water absorption %     |         |       |       | 10.34   |
| Compressive Strength (kg/cm <sup>2</sup> ) | Untreated                          | 108     | 107   | 108   | 108     |
|  | Treated with Wacker OH 100         | 203     | 199   | 189   | 197     |
|  | Increase in compressive strength % |         |       |       | 72.41   |
|  | Treated with MTMOS                 | 215     | 224   | 229   | 211.66  |
|  | Increase in compressive strength % |         |       |       | 95.98   |
|  | Treated with Estel 1000            | 189     | 194   | 198   | 193     |
|  | Increase in compressive strength % |         |       |       | 78.70   |
|  | Treated with Nano Estel            | 113     | 115   | 109   | 112.33  |
|  | Increase in compressive strength % |         |       |       | 4.01    |

[TABLE 4]: Physical and mechanical properties of experimental sandstone samples.

©Done by researcher

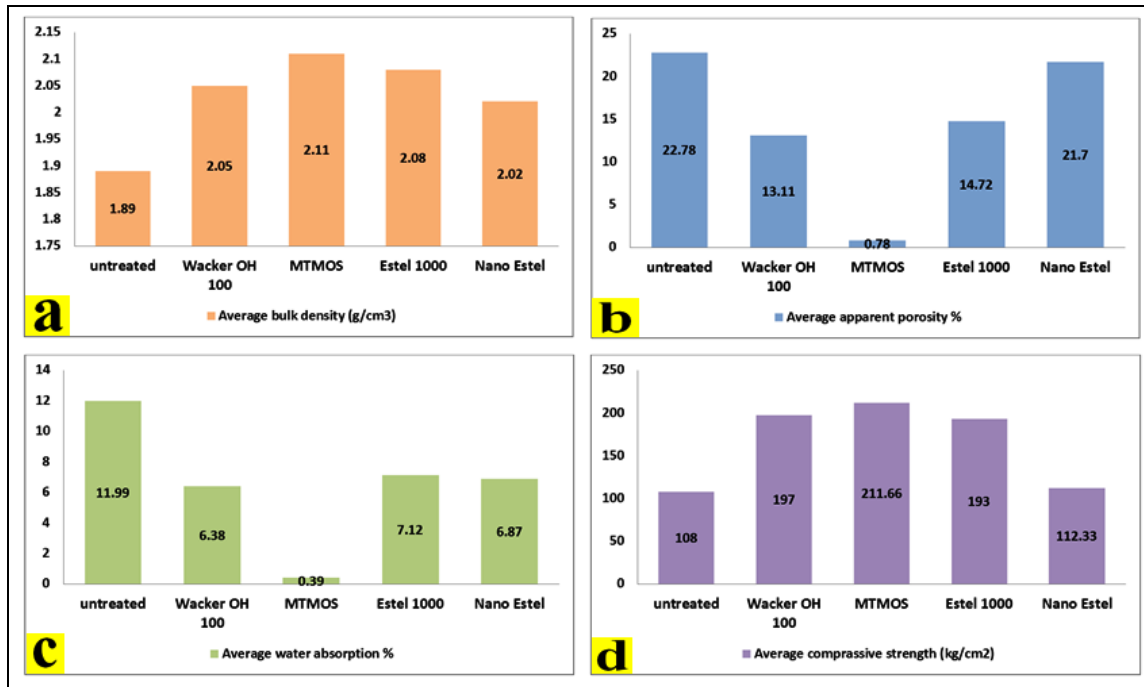


[FIGURE 10]: The physical and mechanical properties of experimental sandstone samples. A) The average bulk density; B) The average apparent porosity; C) The average water absorption; D) The average compressive strength (kg/cm<sup>2</sup>).

### 3. Color Alteration

According to guidelines for conservation purposes of historical or monumental surfaces, the  $\Delta E$  value (total colour variation) of the treated surfaces must be  $< 5$ <sup>36</sup>. The values obtained from chromatic changes measurements  $\Delta E^*_{ab}$  of experimental sandstone samples (treated and untreated) are summarized in [TABLE 5].

| Samples                    | L*    | a*   | b*    | $\Delta E^*$ |
|----------------------------|-------|------|-------|--------------|
| Untreated                  | 71.13 | 6.60 | 17.86 |              |
| Treated with Wacker OH 100 | 63.63 | 7.20 | 20.65 | 8.02         |
| Treated with MTMOS         | 70.76 | 6.20 | 20.25 | 2.45         |
| Treated with Estel 1000    | 69.37 | 7.37 | 23.34 | 5.18         |
| Treated with Nano Estel    | 72.56 | 5.81 | 20.65 | 2.57         |

[TABLE 5]: Results of the chromatic measurements of the treated sandstone samples © Done by researcher

The samples treated by MTMOS achieved lowest value of total color change  $\Delta E^*_{ab}$  (2.45), which is below the threshold values according to guidelines for conservation purposes. Also the samples treated with Nano Estel has  $\Delta E^*_{ab}$  (2.57), which also did not exceed guidelines values of conservation purposes. But the Estel 1000 product caused a minor change in the colour of treated sandstone samples, achieved a value of  $\Delta E^*_{ab}$  (5.18), while Wacker OH 100 product failed to conserve the natural color of treated samples,

<sup>36</sup> GIOVANNI et Al 2015: 222-231; NORMAL 2017; FRANCESCA et Al 2018: 1-23.

causing significant alteration in color of treated sandstone samples. It achieved the highest value of total color change  $\Delta E^*ab$  (8.02), exceeding guidelines values of conservation purposes.

#### 4. Static water contact angle

To evaluate the water repellency of the treated samples, the static contact angle (sessile drop method) of water droplets placed on different positions on the samples were measured, and the average values were taken. The untreated and treated samples were included in this test for comparison. The results showed that all consolidants used in this study enhanced the property of water repellency of the sandstone samples, as shown in [FIGURE 11]. MTMOS product achieved the highest static water contact angle value ( $104^\circ$ ), [FIGURE 11/A], so it considered as a hydrophobic material because it has achieved contact angles more than 90 degrees. The hydrophobicity of this consolidant may be as a result of containing a non-polar methyl group connecting to the silicon atoms that form main chain of this polymer<sup>37</sup>. Estel 1000 product had static water contact angle value ( $74.6^\circ$ ), [FIGURE 11/B]. While Wacker OH 100 product had static water contact angle value ( $37.9^\circ$ ), [FIGURE 11/C]. Nano Estel product had achieved the static water contact angle value ( $15^\circ$ ), which is suggested to be ascribed to the high surface tension of the consolidation material in addition to the cracked and dense microstructural network formed on the treated stone surface. [FIGURE 11/D]. Therefore, Estel 1000, Wacker OH 100 and Nano Estel are considered hydrophilic materials, as they achieved water contact angles less than 90 degrees.

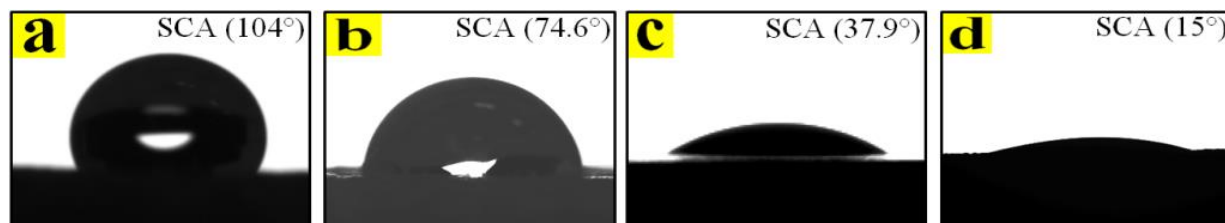


[FIGURE 11]: Photographs of water droplets on the treated sandstone samples; A) MTMOS treatment; B) Estel 1000 treatment; C) Wacker OH 100 treatment; D) Nano Estel treatment.

### C. Evaluation of the Mortars

#### 1- Visual Appearance

By Visual examination to the surficial appearance of the prepared mortars to choose the most appropriate one for filling gaps and joints in the main facades of the temple after drying and setting, the following notes have been observed [FIGURE 12]:

- Mortar (A) is clear white in color, fine texture and appears to be strong and very cohesive, which is incompatible with the sandstone used for the temple's main facades. The amount of lime used may be the cause of the mortar's white tint.
- Mortar (B) is too weak, too fragile, easy to scratch, has homogeneous texture, dark gray color, which is incompatible with the sandstone used for the temple's main facades.

<sup>37</sup> HELMI et Al 2016: 29-40.

- Mortar (C) is strong, has good cohesion, has homogeneous texture and is compatible in color with the sandstone used for the temple's main facades.
- Mortar (D) matches the color and texture of the main temple facades' sandstone but is too strong, has high cohesiveness, and homogeneous texture.

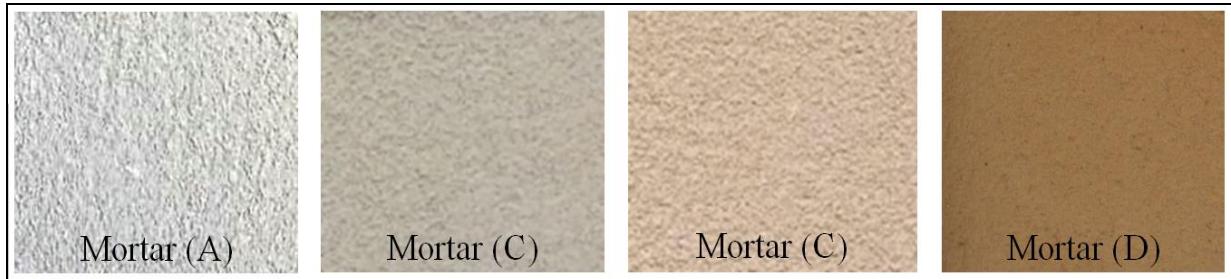


[FIGURE 12]: General appearance of the mortars samples.

## 2. Physical and Mechanical Properties

The results of physical and mechanical properties of prepared mortars were reported in [TABLE 6]. In a comparison, it was found that the mortar (C) achieved the best results in terms of physical and mechanical properties. It has the highest bulk density  $1.78 \text{ gm/cm}^3$ , the lowest average values of apparent porosity, amount to 4.37%, the lowest average values of water absorption 2.45%, and the highest average values of compressive strength  $109.39 \text{ kg/cm}^2$ . This is may be attributed to the granular gradation of the components, which led to a good incorporation of the mortar, in addition to the ratio of mortar components, and the role of the (Eucopor M) product. From the above mentioned results it was decided that the mortar (A) would be the suitable mortar for filling gaps and joints in the external facades of the temple at Medinet Habu, as shown in [FIGURE 13].

| Mortar name | Bulk density ( $\text{g/cm}^3$ ) | Apparent porosity (%) | Water absorption (%) | Compressive Strength ( $\text{kg/cm}^2$ ) |
|-------------|----------------------------------|-----------------------|----------------------|---|
| (A)         | 1.64                             | 32.54                 | 16.22                | 94.25                                     |
| (B)         | 1.67                             | 38.32                 | 18.87                | 75.68                                     |
| (C)         | 1.78                             | 4.37                  | 2.45                 | 109.39                                    |
| (D)         | 1.73                             | 6.25                  | 3.61                 | 105.21                                    |

[TABLE 6] :Physical and mechanical properties of mortars samples© Done by researcher

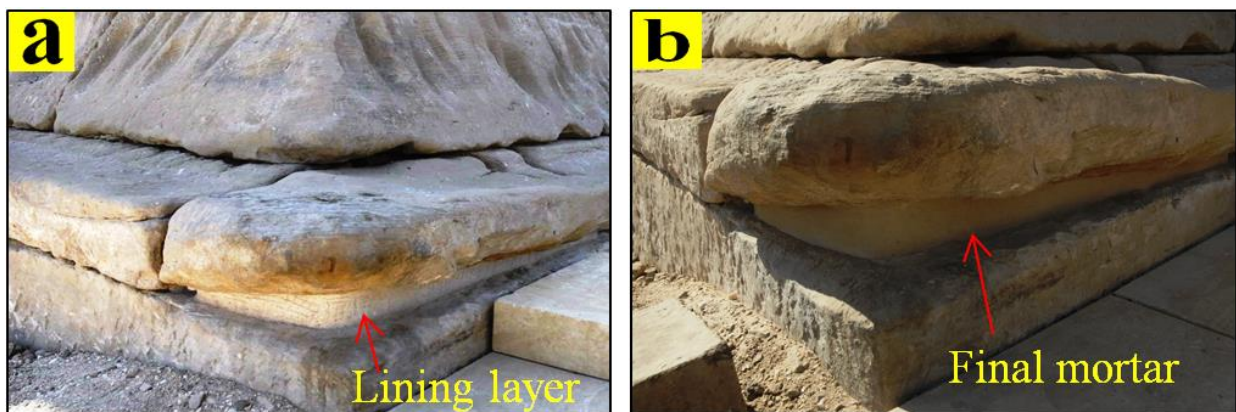


[FIGURE 13]: Filling joint in the external facades of the mortuary temple at Medinet Habu using mortar; A) after applying the lining layer of mortar; B) after applying the final mortar above of the lining.

#### IV. CONCLUSIONS

Observation and visual examination reveal different kinds of deterioration phenomena to the inscriptions on the external facades of the temple, such as scaling, flaking, powdering, discoloration, cracking, gaps, open joints, fragmentations, bird droppings, salt efflorescence, and scratches (blessing marks). The main factors contributing to the deterioration of these wall reliefs are the rising salty ground water level in the temple area, caused by unplanned urban and agricultural encroachments, human actions, and biodeterioration factors, particularly the wild pigeons. According to the results of investigation and analytical study, the main facades of the mortuary temple at Medinet Habu was built of Nubian sandstone, most probably from Gebel El- Silsila quarry. It consists mainly of sub rounded to angular very fine to medium and sorted grains of quartz, in addition to minor amounts of kaolinite  $Al_2(OH)_4Si_2O_5$ , calcite  $CaCO_3$  and halite NaCl. Moreover, rare amounts of biotite, feldspars, zircon, iron oxides, opaques. Also, the archaeological mortar consists mainly of gypsum  $CaSO_4 \cdot 2H_2O$ , fragments of carbonate rock in micrite form (calcite  $CaCO_3$ ), quartz  $SiO_2$  and halite NaCl. It is suggested that the presence of halite in the composition of the studied archaeological sandstone and mortar samples is considered as one of the weathering products. The results of experimental study of the cleaning poultices revealed that the poultice (A) is threefold effective than the poultice (B), as it easily removes dirt, stains and bird droppings from the inscriptions surfaces on the external facades of the studied temple. Also, the results of experimental study demonstrated that the (Dow Corning MTMOS) Methyltrimethoxysilane is the most suitable product for the consolidation and protection of the inscriptions on the main facades of the studied temple, as it achieved the best amelioration values of the mechanical and physical properties of the treated sandstone samples. Moreover, it showed good hydrophobic properties, as it achieved the highest values of static water contact angle. In addition, it achieved an excellent distribution and formed a homogeneous coating on the stone surface without closing the pores, as observed by SEM microscopic investigation. It didn't cause any effect on the color or the general appearance of the treated sandstone samples. In addition; the experimental study of prepared mortars revealed that the mortar (C) is more suitable than other studied mortars for filling gaps, as it is compatible in terms of physical, mechanical and optical properties with archaeological sandstone in the main facades of the temple.

The achieved results in this study will be useful for conservation of the wall reliefs on the main facades of the mortuary temple at Medinet Habu.

#### V. ACKNOWLEDGEMENTS

The author is very grateful to Prof. Dr. Adel Akarish from Geological Sciences Dept., National Research Centre, Cairo, Egypt, for his scientific assistance in this research and all the members of Medinet Habu site, for their assistance during collecting the archaeological information of the site, and also for permission to study the inscriptions on the external facades of the mortuary temple at Medinet Habu.

## BIBLIOGRAPHY

- AHMED, M.A., ALI, M.F., BADER, N.A. & KHALAPHALLAH, R.: «The Effect of Wild Pigeon Excreta on the Wall Painting of Ramses III Temple at Medinet Habu, Luxor», *Scientific Culture* 7/3, 2021, 53-63.
- ASTM C 170.: «American Society for Testing and Protection of Stone Monuments. Standard Test Methods for Compressive Strength of Natural building stone, ASTM C 170», UNESCO, Paris, 1976.
- AYMAN, A. AHMED & GRAHAM, E. FOGG.: «The Impact of Groundwater and Agricultural Expansion on the Archaeological Sites at Luxor, Egypt», *Journal of African Earth Sciences* 95, 2014, 93-104.
- BADER, N.A & ABU EL-HASSAN, R.: «Examination and Conservation of Helal El-Beah Mosque, Dakahlia, Egypt», *Journal of Building Construction and Planning Research* 4/2, 2016, 103-118. DOI: 10.4236/jbcpr.2016.42007
- BADER, N.A & ASHRY, A.M.: «The Cleaning of the Isis Temple's Mural Paintings in Upper Egypt Using Zinc Oxide Nanoparticles and Non-ionic Detergent», *International Journal of Conservation Science* 7/2, 2016, 443-458.
- BADER, N. A.: «The Deterioration Problems of the Wall Reliefs of Komir Temple, Esna, Egypt», *Mediterranean Archaeology & Archaeometry* 14/1, 2014, 201-219.
- BAGLIONI, P., CHELAZZI, D. & GIORGI, R.: *Nanotechnologies in the Conservation of Cultural Heritage A compendium of materials and techniques*, Springer Science & Business Media Dordrecht, 2015, 6. DOI 10.1007/978-94-017-9303-2
- BALA'AWI, F., ALSHAWABKEH, Y., AL MASRI, E. & MUSTAFA, M.: «Salt Damage and Environmental Conditions: A Thermodynamic Approach from The Northern Roman Theater in Jerash, Jordan», *Mediterranean Archaeology and Archaeometry* 18/2, 2018, 49-66.
- BALKSTEN, K.: «Understanding Historic Mortars and their Variations a Condition for Performing Restorations with Traditional Materials», 2010, <https://www.researchgate.net/publication/292041695>
- BENAVENTE, D., GRACIA DEL CURA, M., GRACIA-GUINEA, J., SÁNCHEZ-MORAL, S. & ORDÓÑEZ, S.: «Role of Pore Structure in Salt Crystallization in Unsaturated Porous Stone», *Journal of Crystal Growth* 206, 2004 532-544.
- CAI, X., ZHOU, Z., LIU, K., DU, X. & ZANG, H.: «Water Weakening Effects on the Mechanical Behaviour of Different Rock Types: Phenomena and Mechanisms», *Applied. Sciences* 9, 4450, 2019, 1-18.
- CHIAKI, T. OGUCHI & SWE YU.: «A Review of Theoretical Salt Weathering Studies for Stone Heritage», *Progress in Earth and Planetary Science* 8/32, 2021, <https://doi.org/10.1186/s40645-021-00414-x>
- CIE STANDARD.: Colorimetry, part 4: CIE 1976 L\*a\*b\* colour space, *International Standard*, 1<sup>st</sup> ed. , 2019-06.
- DARWISH, S.S.: «Evaluation of The Effectiveness of Some Consolidants Used for The Treatment of The XIXTH Century Egyptian Cemetery Wall Painting», *International Journal of Conservation Science* 4/4, 2013, 413-422.
- DESARNAUD, J. DERLUYN, H., MOLARI, L., DE MIRANDA, S., CNUUDE, V. & SHAHIDZADEH, N.: «Drying of Salt Contaminated Porous Media: Effect of Primary and Secondary Nucleation», *Journal of Applied Physics* 118/11, 114901, 2015, 1-10, <https://doi.org/10.1063/1.4930292>
- DZIEDZIC, T., BARTZ, W. & GAŚSIOR, M.: «Mineralogical Characteristic of Mortars from the Temple of Hatshipsut at El Deir el Bahari: Preliminary Report», *Polish Centre of Mediterranean Archaeology* 24/2, University of Warsaw, Warszawa, 2015, 39-111.
- EL-DERBY, A., MANSOUR, M. & SALEM, M.: «Investigation the Microbial Deterioration of Sandstone from the Osirion Sarcophagus Chambers as Affected by Rising Ground Water Level», *Mediterranean Archaeology and Archaeometry*, 16/1, 2016, 273-281.
- ELFADALY, A., ATTIA, W. & LASAPONARA, R.: «Monitoring the Environmental Risks Around Medinet Habu and Ramesseum Temple at West Luxor, Egypt, Using Remote Sensing and GIS Techniques», *Journal of Archaeol Method Theory* 25, 2018, 587-610.
- ELFADALY, A., Wafa. O., ABOUARAB, M., GUIDA, A., SPANU, P. & LASAPONARA, R.: « Geo-Environmental Estimation of Land Use Changes and Its Effects on Egyptian Temples at Luxor City», *ISPRS Int. J. Geo-Inf* 6/11, 2017, 378, <https://doi.org/10.3390/ijgi6110378>
- EL-GOHARY, M.: «Effective Roles of Some Deterioration Agents Affecting Edfu Royal Birth House «Mammisi»», *International Journal of Conservation Science* 6/3, 2015, 349-368.
- Eppes, M. & Keanini, R.: «Mechanical Weathering and Rock Erosion by Climate-Dependent Subcritical Cracking», *Reviews of. Geophysics* 55/2, 2017, 470-508.
- FERNANDEZ, A.S., VILLALBA, L.S., RABANAL, M.E. & FORT, R.: «New Nanomaterials for Applications in Conservation and Restoration of Stony Materials: A review», *Materiales de Construcción* 67/325, 2017, 1-18.
- FERREIRA, A. PINTO & DELGADO, J. RODRIGUES.: «Stone Conservation: The Role of Treatment Procedures», *Journal of Cultural Heritage* 9, 2008, 38-53.

ASSESSING CONSERVATION TREATMENTS OF THE MAIN FAÇADES OF  
MEDINET HABU TEMPLE, LUXOR-EGYPT

- FITZNER, B., HERINRICHS, K., LA BOUCHARDIERE, D.: «Weathering Damage on Pharaonic Sandstone Monuments in Luxor- Egypt», *Building and Environment* 38, 2003,1089 -1103.
- FRANCESCA, P., ANTONELLA, P., ALESSANDRA, T., MARIATERESA, L., MAURIZIO, M., ANGELA, C., LUCIA, M.C & ROBERTO, C.: «TiO<sub>2</sub> Nanocrystal Based Coatings for the Protection of Architectural Stone: The Effect of Solvents in the Spray-Coating Application for a Self-Cleaning Surfaces», *Coatings* 8/10, 2018, 356. DOI: 10.3390/coatings8100356
- GABRIELA, G., ENRICO, S. & ELISA, F.: «Consolidation of Porous Carbonate Stones by an Innovative Phosphate Treatment: Mechanical Strengthening and Physical Microstructural Compatibility in Comparison with TEOS based treatments», *Heritage Science* 3/1, 2015, 1:6.
- GAJDOS, L., SPERL, M., SLIZKOVA, Z. & DRDLOVA, M.: «The Effect of Consolidation Treatment on Selected Mechanical Properties of Sandstone», *IOP Conf. Series: Materials Science and Engineering* 1205, 2021, 1-11.
- GEORGE, W. & ELIZABETH, S.GOINS.: *Alkoxysilanes and the Consolidation of Stone*, Research in Conservation, *The Getty Conservation Institute* (Getty Publications) 2005, 1-14.
- GERMINARIO, L. & OGUCHI, C.T.: «Underground Salt Weathering of Heritage Stone: Lithological and Environmental Constraints on the Formation of Sulfate Efflorescences and Crusts», *Journal of Cultural Heritage* 49, 2021, 85–93.
- GIOVANNI, B.G. & PLACIDO, M.: «Preservation of Historical Stone Surfaces by TiO<sub>2</sub> Nanocoatings», *Coatings* 5, 2015, 222-231.
- GUPTA, S.P., RANA, K.S., SHARMA, D.N. & CHANDROL, G.K.: « Diversity and Index of Similarity of Microorganisms on Sandstone with Special Reference to Historical Monuments of Chhattisgarh, India», *International Journal of Current Microbiology and Applied Sciences* 2/12, 2319-7706, 2013, 51-57.
- HADI, A. & ALI, M.: «The Effect of Grain Size and Cement Content on Index Properties of Weakly Solidified Artificial Sandstones», *Journal of Geophysics and Engineering* 15/2, 2018, 613–619. <https://doi.org/10.1088/1742-2140/aaa14a>
- HARRELL, J.A. & STOREMYR, P.: «Ancient Egyptian Quarries—an Illustrated Overview», *Geological Survey of Norway Special Publication* 12, 2009, 7–50.
- HASSAN, L. KH.: «Reintegration Technique (Missing Parts): In Conservation-Restoration of Antiquities», *International Journal of Archaeology* 10/2, 2022, 38-45. DOI: 10.11648/J.IJA.20221002.12.
- HEFNI, Y. K.: «Hydrophobic Zinc Oxide Nanocomposites for Consolidation and Protection of Quartzite Sculptures: A Case Study», *Journal of Nano Research* 63, 2020, 64-75. <https://doi.org/10.4028/www.scientific.net/JNanoR.63.64>
- HELMI, F.M. & HEFNI, K.Y.: «Nanocomposites for the Protection of Granitic Obelisks at Tanis, Egypt», *Mediterranean Archaeology and Archaeometry* 16/2, 2016, 87-96.
- HELMI, F.M. & HEFNI, Y.K.: «Using Nanocomposites in the Consolidation and Protection of Sandstone», *International Journal of Conservation Science* 7/1, 2016, 29-40.
- HEMEDA, S., KHALIL, M., SHOEB, A. & ABD EL AZIZ, A.: «The Effectiveness of Nano Materials and Nano- Modified Polymers for Preservation of Historic Brick Masonry in Rashid, Egypt», *International Journal of Conservation Science* 9/4, 2018, 835-846.
- HÖLSCHER, U.: *The Mortuary Temple of Ramses III, Part I. The Excavation of Medinet Habu*, vol.3, Chicago (The University of Chicago Press) 1941.
- HOSSAM, I.: «The Climate and its Impacts on Egyptian Civilized Heritage: EI-Nadura Temple in El-Kharga oasis, Western Desert of Egypt as a Case Study», *Journal of Geography and Earth Sciences* 3/2, 2015, 67-82. DOI: 10.1515/pesd-2015-0001
- JCPDS.: Joint Committee on Powder Diffraction Standards, Index to the Powder Diffraction File, *American Society for Testing and Materials, Pennsylvania* (THE PUBLISHER) 1967.
- JOSÉ DAS CANDEIAS SALES.: «The Smiting of the Enemies Scenes in the Mortuary Temple of Ramses III at Medinet Habu, Oriental Studies», *Journal of Oriental and Ancient History* 1, 2012, 87.
- LABUS, M. & BOCHEN, J.: «Sandstone Degradation: An Experimental Study of Accelerated Weathering», *Environ Earth Sciences* 67, 2012, 2027–2042.
- LAMP, J., MARCHANT, D., MACKAY, S. & HEAD, J.:« Thermal Stress Weathering and the Spalling of Antarctic rocks», *Journal of Geophysical Research: Earth Surface* 122/1, 2017, 3-24. <https://doi.org/10.1002/2016JF003992>
- LICCIULLI, A., CALIA, A., LETTIERI, M. & et Al.: «Photocatalytic TiO<sub>2</sub> Coatings on Limestone», *Journal of Sol-Gel Science and Technology* 60/3, 2011, 437–444.



- MAHMOUD, H.M, KANTIRANIS, N. & STRATIS, J.: «Salt Damage on the Wall Paintings of the festival temple of Thutmosis III, Karnak temple complex, Upper Egypt. A Case Study», *International Journal of Conservation Science* 1/3, 2010, 133-142.
- EL ATTAR, MANSOUR, A.: «Assessment of Salt Damage Based on Crystallization Test Due to High Groundwater Level in Sandstone Monuments, Luxor, Egypt», *International Journal of Scientific & Engineering Research* 10/11, 2019, 1352-1360.
- MARCO, L. MARQUES & CARLOS, C.: «Consolidation Works on Sandstone Monuments A new approach», *Handbook of Materials Failure Analysis*, 2018, 235-254. <http://dx.doi.org/10.1016/B978-0-08-101928-3.00012-4>.
- MARTINEZ, J. M., TORRERO, E & SANZ, D.: «Salt Crystallization Dynamics in Indoor Environments: Stone Weathering in the Muñoz Chapel of the Cathedral of Santa María (Cuenca, central Spain)», *Journal of Cultural Heritage* 47/4, 2021, 123-132. DOI:10.1016/j.culher.2020.09.011.
- MISCEVIC, P. & VLASTELICA, G.: «Impact of Weathering on Slope Stability in Soft Rock Mass», *Journal of Rock Mechanics and Geotechnical Engineering* 6/3, 2014, 240-250. <https://doi.org/10.1016/j.jrmge.2014.03.006>
- MOHAMMAD, A. ALDOSARI, SAWSAN, S. DARWISH., MAHMOUD, A. ADAM., NAGIB, A. ELMARZUGI & SAYED, M. AHMED.: «Evaluation of Preventive Performance of Kaolin and Calcium Hydroxide Nanocomposites in Strengthening the Outdoor Carved Limestone», *Archaeological and Anthropological Sciences* 11, 2019, 3389–3405.
- MOUSSA, A., BADAWEY, M., & SABER, N.: «Chromatic Alteration of Egyptian Blue and Egyptian Green Pigments in Pharaonic Late Period Tempera Murals», *Scientific Culture* 7/2, 2021, 1-15. DOI: 10.5281/zenodo.4465458
- MOUSSA, A.: «Assessing the Decay Agents of Wall Paintings in Al Qurna and Wadi El Natrun Regions-Egypt», PhD thesis, Lab. of Engineering Geology and Hydrogeology, Department. of Geology, Faculty of Science, Aristotle University of Thessaloniki, Greece, 2007.
- MOUSSA, A., KANTIRANIS, N., VOUDOURIS, K., STRATIS, J., ALI, M & CHRISTARAS, V.: « Impact of Soluble Salts on the Deterioration of Pharaonic and Coptic Wall Paintings in Al Qurna, Egypt: Mineralogy and Chemistry», *Archaeometry* 51 /2, 2009, 292-308. DOI: 10.1111/j.1475-4754.2008.00422.x
- MOUSSA, A., VOUDOURIS, K., STRATIS, J., ALI, M. & CHRISTARAS, B.: «Assessing The Deterioration of Frescoes Using Hydrogeochemical and Geological Data: Two Examples from Egypt», *Water and Cultural Heritage" the 7th International Symposium on the Conservation of monuments in the Mediterranean Basin*, 6-9 June, Orléans, France, 2007.
- MURNANE, W. J.: *United with Eternity: A Concise Guide to the Monuments of Medinet Habu*, Chicago (The University of Chicago Press) 1980.
- NELSON, H., EDGERTON, W., WILLIAMS, C., WILSON, J., BOLLACHER, A., CANZLAVI, N., CHUBB, J., MORRISON, A., LIND, O & HARTMAN, J.: *Earlier Historical Records of Ramses III*, Chicago (The University of Chicago Press) 1930.
- NICHOLSON, P. & SHAW, I.: *Ancient Egyptian Materials and Technology*, Cambridge (Cambridge University Press) 2000.
- NORD, A.G. & Ericsson, T.: «Chemical Analysis of Thin Black Layers on Building Stone», *Studies in Conservation* 38/1, 1993, 24-35.
- NORMAL, R.: «Misura Colorimetrica Strumentale di Superfici Opache», 2017, [http://www.architettilroma.it/fpdb/consultabc/File/ConsultaBC/Lessic\\_NorMal-Santopuoli.pdf](http://www.architettilroma.it/fpdb/consultabc/File/ConsultaBC/Lessic_NorMal-Santopuoli.pdf). Accessed on 02/08/ 2017.
- ORABI, E.A. & ABU ELYAMEEN, A.: «Analytical Study and Treatments of the Decayed Mural Paintings at Athribis in Sheikh Hamad Temple, Sohag governorate, Egypt», *SHEDET* 7, 2020, 238-249. DOI: 10.21608/SHEDET.2020.32147.1015
- PESCE, C., MORETTO, L., ORSEGA, E., PESCE, G., MARCO CORRADI, & WEBER, J.: «Effectiveness and Compatibility of a Novel Sustainable Method for Stone Consolidation Based on Di-Ammonium Phosphate and Calcium-Based Nanomaterials», *Materials* 12/18, 2019, 3025. <https://doi.org/10.3390/ma12183025>
- REMZOVA, M., ZOUZELKA, R., LUKES, J. & RATHOUSKY, J.: «Potential of Advanced Consolidants for the Application on Sandstone», *Appl. Sci.* 9/23, 2019, 5252. <https://doi.org/10.3390/app9235252>
- RODRIGUES, D.J.: «Consolidation of Decayed Stones. A Delicate Problem with Few Practical Solutions», *Proc. Int. Seminar on Historical Constructions*, 2001, 3- 14. *Research Gate*
- RUFFOLO, S.A., LA RUSSA, M.F., ALOISE, P., BELFIORE, C. M. & et AL.: «Efficacy of Nanolime in Restoration Procedures of Salt Weathered Limestone Rock», *Applied Physics A, Materials Science & Processing* 114, 2013, 753-758.

*ASSESSING CONSERVATION TREATMENTS OF THE MAIN FAÇADES OF  
MEDINET HABU TEMPLE, LUXOR–EGYPT*

- SALEH, I., ABDEL HADY, M., MOUSSA, A., HEFNI, Y., ABD EL-LATIF, M.: «Experimental Study for the Consolidation and Protection of Sandstone Petroglyphs at Sarabit el Khadam (Sinai, Egypt) », *Scientific Cultural* 5/1, 2019, 43-48. DOI: 10.5281/zenodo.1451906
- SCOTT, M. PETERS.: «Decoding the Medinet Habu Inscriptions: The Ideological Subtext of Ramesses III's War Accounts», BA Thesis, *Columbia College, Columbia University*, 2011. <https://doi.org/10.7916/D89G5TT7>
- SIEGISMUND, S. & SNETHLAGE, R.: *Stone in Architecture Properties, Durability Fourth 4<sup>ed.</sup>*, Berlin (Springer-Verlag Berlin Heidelberg) 2011.
- SMITH, B.J., GOMEZ-HERAS, M., MENEELY, D. & et Al.: «High Resolution Monitoring of Surface Morphological Change of Building Limestones in Response to Simulated Salt Weathering», *Proceedings of 11<sup>th</sup> International Congress on Deterioration and Conservation of Stone 1*, Torun, 2008, 275-282.
- SPENNEMANN, D.H. & WATSON, M. J.: «Experimental Studies on the Impact of Bird Excreta on Architectural Metals. APT Bulletin», *Journal of Preservation Technology* 49/1, 2018, 19-26.
- SPENNEMANN, D.H., PIKE, M. & WATSON, M.J.: «Effects of Acid Pigeon Excreta on Building Conservation», *International Journal of Building Pathology and Adaptation* 35/1, 2017, 2-15. <https://doi.org/10.1108/IJBPA-09-2016-0023>.
- SPENNEMANN, D., PIKE, M. & WATSON, M. J.: «Behaviour of Pigeon Excreta on Masonry Surfaces», *Restoration of Buildings and Monuments* 23/1, 2017, 15-28, <http://dx.doi.org/10.1515/rbm-2017-0004>
- SWANN, J.: «Modes of decay, Conservation», *Discovering Stone* 20, 24-29, [www.infotile.com/publications](http://www.infotile.com/publications)
- TORRES, I.: «New Technique for Treating Rising Damp in Historical Buildings: Wall Base Ventilation», *Journal of Cultural Heritage* 31, 2018, 560-570. <https://doi.org/10.1016/j.culher.2018.04.015>.
- VEREZEN, V.: «The Crumbling Wonder: A Damage and Risk Assessment of Sandstone Monuments and Natural Features in the Petra Archaeological Park, Jordan», *Journal of Student Research in Archaeology* 3, 2017, 20-34.
- WÜST, R. & SCHLÜCHTER, C.: «The Origin of Soluble Salts in Rocks of the Thebes Mountains, Egypt: The Damage Potential to Ancient Egyptian Wall Art», *Journal of Archaeological Science* 27/12, 2000, 1161-1172. <https://doi.org/10.1006/jasc.1999.0550>
- YALDIZ, E.: «Climate Effects on Monumental Buildings», *Research Gate*, Balwois, Ohrid, Republic of Macedonia, 2010, 1-10, [https://www.researchgate.net/publication/319136948\\_Climate\\_Effects\\_on\\_Monumental\\_Buildings](https://www.researchgate.net/publication/319136948_Climate_Effects_on_Monumental_Buildings)
- YASER, Y. ABDEL-ATY, HASSAN, S. MAHMOUD & ABDULNASER, A. AL-ZAHRANIC.: «Experimental Evaluation of Consolidation Techniques of Fossiliferous Limestone in Masonry Walls of Heritage Buildings at Historic Jeddah, Kingdom of Saudi Arabia», *Advanced Research in Conservation Science* 1/1, 2020, 16-33. DOI: 10.21608/ARCS.2020.111205
- YÜKSEK, S.: «Mechanical Properties of some Building Stones from Volcanic deposits of Mount Erciyes (Turkey) », *Materiales de Construcción* 69/334, 2019, 1-13. <https://doi.org/10.3989/mc.2019.04618>.
- ZHIXUE, S., ZHILEI, S., HONGJIANG, L., XIJIE, Y. & YONG, Y.: «Characteristics of Carbonate Cements in Sandstone Reservoirs: A Case from Yanchang Formation, Middle and Southern Ordos Basin, China», *PETROL EXPLOR& DEVELOPMENT* 37/5, 543-551. [https://doi.org/10.1016/S1876-3804\(10\)60054-7](https://doi.org/10.1016/S1876-3804(10)60054-7)